

VLBI Observations of the Blazar 1611+343 at 5 GHz

Tao An*, Xiao-Yu Hong, Wei-Hua Wang, Dong-Rong Jiang and Yong-Jun Chen

Shanghai Astronomical Observatory, Chinese Academy of Sciences, Shanghai 200030
National Astronomical Observatories, Chinese Academy of Sciences, Beijing 100012

Received 2001 March 25; accepted 2001 June 20

Abstract The gamma-ray blazar 1611+343 was observed with polarization VLBI mode at 5 GHz in February 1999. The total intensity (I) VLBI image of the source shows a core-jet structure. The jet bends eastward at ~ 3 mas south of the core. Four components have been detected from results of fitting, with apparent speeds estimated at 6.7 ± 0.7 , 2.5 ± 0.3 , $4.5 \pm 0.5 h^{-1}c$ for three jet components (taking $H_0 = 100 h \text{ km s}^{-1} \text{ Mpc}^{-1}$, $q_0 = 0.5$). The polarization (P) VLBI image of 1611+343 displays the polarized configuration in the jet. The mechanism of the curved jet is discussed.

Key words: galaxies: blazar: individual — radio continuum: galaxies

1 INTRODUCTION

The radio source 1611+343 was identified as an optically violent variable quasar (OVV) with $z = 1.401$ (Herwitt & Burbidge 1989). This blazar is among the high-energy gamma-ray blazars which are detected by EGRET (Energetic Gamma Ray Experiment Telescope). It is commonly thought that the gamma-ray is produced from inverse Compton scattering of the synchrotron photons by relativistic electrons, i.e., synchrotron self-Compton (SSC) emission in a beamed relativistic jet. Hence sources that contain relativistic jets show distinct properties such as apparent superluminal motion and, in fact, several do. 1611+343 is one of the EGRET sources displaying distinct apparent superluminal motion.

A VLA image of high dynamic range displayed a triple morphology (Murphy & Browne 1993) at arcsecond scale. There were three components in the VLA image; in addition to the presumed core, there were two other components: one was at 5 arcsecond from the core at P.A. $\sim 193^\circ$; the other, 10 arcsecond north from the core at P.A. $\sim 10^\circ$. The double-lobe structure of the source showed that it is an aligned source at arcsecond scale. VLBI observations at low frequencies revealed 1611+343 as a compact component (Romney et al. 1984; Padrielli et al. 1986, 1991; Bondi et al. 1996), while high resolution VLBI observations showed the source had a core-jet configuration with several jet components (Piner & Kingham 1997, hereafter PK 97, Matthew L. Lister and Alan P. Marscher 1998, hereafter LM 98, Jorstad et al. 2000, hereafter

* E-mail: antao@center.shao.ac.cn

Jorstad 2000). Piner & Kingham (1997) presented multi-epoch images of the source at 8 GHz and fitted the source with 5 components. The apparent superluminal speeds of four of the components, which were detected from the 8 GHz VLBI data, are 6.7 ± 1.6 , 3.8 ± 1.4 , 7.6 ± 1.3 , and $11.5 \pm 2.3 h^{-1}c$ for C1, C2, C3 and C5, respectively (Piner & Kingham 1997). The source was also observed by LM 98 at 43 GHz and Jorstad 2000 at 43 GHz, 22 GHz and 15 GHz.

In this paper we will present the I and P VLBI images and estimate the proper motions of the jet components.

2 OBSERVATION AND DATA PROCESSING

The blazar 1611+343 was observed with the EVN (European VLBI Network) at 5 GHz. The observation was carried out with snapshot mode of 7 scans of 13 minutes in February 1999. The participating antennas of the EVN were Effelsberg, WSRT, Jodrell Bank, Cambridge, Onsala, Turun, Shanghai, Urumqi, and Hartebeesthoek. The data were obtained with the MK III VLBI recording system with an effective bandwidth of 28 MHz and correlated at the Max Planck Institut für Radionastronomie MK III correlator in Bonn. Data post-processing including editing, amplitude calibrating, fringe fitting were done by the NRAO Astronomical Image-Processing system (AIPS) software package. The VLBI images were produced using both the DIFMAP (DIFerence MAPping) and AIPS software package. The 5 GHz I VLBI image of 1611+343 is presented in Fig. 1 and the *P* VLBI image is shown in Fig. 2.

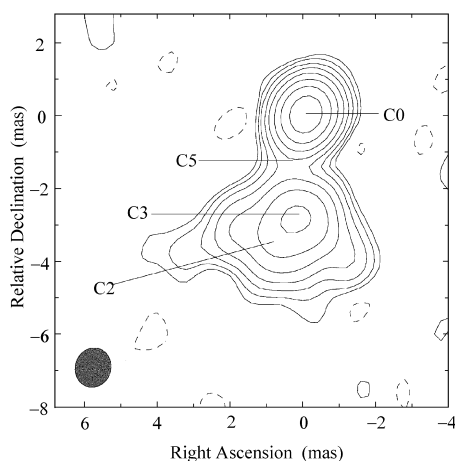


Fig. 1 The VLBI Image of 1611+343 at 5 GHz; Beam FWHM: 1.09×0.98 (mas) at -17°

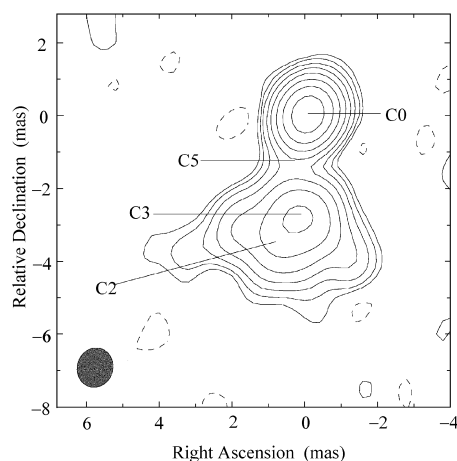


Fig. 2 The polarization VLBI image of 1611+343 at 5 GHz; Beam FWHM: 6.0×3.2 (mas) at -39.5° ; Pol line 1 arcsec = 83.3 Jy/beam; Peak flux = 0.1 Jy/beam; Levs = $0.04 \times (-1, 1, 1.4, 1.8, 2.2, 2.4)$ Jy/beam

3 RESULTS AND ANALYSIS

Figure 1 reveals the core-jet configuration of 1611+343. The jet bends eastward after it is ejected southward through 3 mas. Some physical parameters of the jet components evaluated

through Equations (1)–(9) below are listed in Table 1. The spectra of components C2 and C3, are power-law spectra from the results. The values of β_{app} , apparent transverse velocity, and β , of three jet components support superluminal motion in 1611+343. However, the results of δ_{eq} , the Doppler boosting factor, of C2 are not so large, as a result the calculated position angle exceeds 15° . In addition the brightness temperatures (T_{b}) are far lower than 10^{12} K, the critical temperature of Compton catastrophe.

Table 1 Physical Parameters of Components

Comp.	α^a	β_{app}^b ($h^{-1}c$)	β ($h^{-1}c$)	δ_{eq}	Γ	ϕ ($^\circ$)	T_{b} (10^{12} K)
C5	-0.22	6.7	0.994	2.8	9.5	14.5	0.04
C3	1.86	2.5	0.940	4.1	2.9	12.8	0.06
C2	3.35	4.5	0.996	1.0	10.8	23.7	0.02

^a the spectral indices of C5 and C3 are from the data in Feb. 1999 and in March 1996. The spectral indices of C2 are from the data in Feb.1999 and Oct. 1995.

^b the apparent velocities for C2 and C3 and C5 are gained from our data in Feb. 1999 and PK 97's data in March 1996.

Four components (named C0, C2, C3 and C5) have been identified and tracked by model fitting (Fig. 1). Apparent transverse velocities are estimated for three jet components, 6.7 ± 0.7 , 2.5 ± 0.3 , $4.7 \pm 0.5 h^{-1}c$ for C5, C3 and C2, respectively. These component labels were chosen so as to maintain consistency with PK 97. The spectral index α (defined by $S_\nu \propto \nu^{-\alpha}$) of C0 is measured as -0.05 (a flat and inverted spectrum) between 5 GHz and 8 GHz (PK 97, data of 1996 March), so it is identified as the core of 1611+343; the outmost component is C2; going inward, we have C3, then C5. The component C4 was detected between C5 and C3 in PK 97 at 8 GHz, and a component named B3 (~ 2 mas) was detected between C1 (named by Jorstad 2000, ~ 0.3 mas) and C2 (named by Jorstad 2000, ~ 2.8 mas) in Jorstad 2000 between 1994.76 and 1996.34. The C1 and C2 defined by Jorstad 2000 were described as stationary knots. However, C4 is not detected in our 5 GHz data for lack of sufficient resolution. On one hand, it may be that C4 is too weak to be detected at low resolution at 5 GHz; on the other hand, free-free absorption and synchrotron self-absorption are higher at low frequency than at high frequency, so increasing the difficulty of detecting C4 at 5 GHz. It seems that C3 and C4 are merged into one component (C3) in our 5 GHz image, since there is a slight northward extension from ~ 2 mas south of the core. Thus the distance between models of C3 and C0 (core) will be further shortened, which can influence the computed apparent transverse speed of C3.

Our model fitting results show that the apparent superluminal speed of C3, $2.5 h^{-1}c$, is distinctly lower than in PK 97, at $7.6 \pm 1.3 h^{-1}c$. The velocity of C5 is greater than that of C2, in agreement with the result of PK 97 and Jorstad 2000. This can be the result of different Doppler boosting factors. The viewing angle, ϕ , of C5 is less than that of C2, so the boosting effect of the former is greater than that of the latter. The speed of C3 is lower than the previous result. The first possibility for the decreasing of C3's velocity is that C3 is really slowing down after interacting with the ambient medium. The second possibility is that C4 has merged into C3. The radial distance of C3 is shortened and so the calculated apparent speed is decreased. We tend to accept both possibilities before the true cause is established. All our four components are fitted with elliptical Gaussian models. The model parameters are listed in

Table 2 Gaussian Models

Epoch	Band ^a (GHz)	Com	S^b (Jy)	r^c (mas)	θ (deg)	a^d (mas)	b/a	Φ^e ($^\circ$)
1999	5	C0	1.78	0.00	0.00	0.45	0.42	-33.8
Feb..		C5	0.09	1.22	165.9	0.35	1.00	28.4
...		C3	0.67	2.73	176.6	1.00	0.59	-83.0
		C2	0.92	3.48	169.4	2.52	0.40	83.4
1997.32	15.4	A	2.41 \pm 0.06	0.0 \pm 0.06	...	0.06 \pm 0.04	1.00	...
		F1	0.11 \pm 0.05	0.43 \pm 0.06	+164 \pm 6	0.22 \pm 0.06	1.00	...
		F2	0.09 \pm 0.04	1.48 \pm 0.15	+176 \pm 5	0.42 \pm 0.07	1.00	...
		F3	0.44 \pm 0.08	2.83 \pm 0.18	+178 \pm 6	0.79 \pm 0.08	1.00	...
		G1	0.45 \pm 0.07	3.43 \pm 0.20	+162 \pm 6	1.27 \pm 0.12	1.00	...
1997.32	22.2	A	2.16 \pm 0.05	0.0 \pm 0.04	...	0.05 \pm 0.03	1.00	...
		C1	0.24 \pm 0.04	0.21 \pm 0.08	+168 \pm 5	0.11 \pm 0.04	1.00	...
		B4	0.10	1.26	+176	0.25	1.00	...
		C2	0.29 \pm 0.06	2.83 \pm 0.10	+178 \pm 4	0.69 \pm 0.05	1.00	...
		B2	0.19 \pm 0.05	3.46 \pm 0.13	+167 \pm 5	0.97 \pm 0.06	1.00	...
		B1	0.11 \pm 0.06	3.71 \pm 0.20	+157 \pm 6	0.90 \pm 0.08	1.00	...
1997.32	43.2	A	1.65 \pm 0.06	0.0 \pm 0.04	...	0.07 \pm 0.03	1.00	...
		E1	0.25 \pm 0.06	0.16 \pm 0.05	+169 \pm 4	0.11 \pm 0.04	1.00	...
		E2	0.05	0.61	+154	0.22	1.00	...
		E3	0.04	1.45	+176	0.59	1.00	...
		E4	0.04	2.31	+179	0.25	1.00	...
		E5	0.07	2.94	+176	0.31	1.00	...
		D1	0.08	3.29	+166	0.75	1.00	...
1995.31	22.2	A	3.45 \pm 0.05	0.0 \pm 0.04	...	0.07 \pm 0.03	1.00	...
		C1	0.32 \pm 0.05	0.23 \pm 0.10	+161 \pm 6	0.11 \pm 0.03	1.00	...
		B3	0.14	2.00	+178	0.36	1.00	...
		C2	0.26 \pm 0.04	2.78 \pm 0.18	+178 \pm 5	0.63 \pm 0.07	1.00	...
		B2	0.20 \pm 0.06	2.99 \pm 0.20	+161 \pm 5	0.69 \pm 0.09	1.00	...
		B1	0.07	3.16	+169	0.27	1.00	...
1996	8	C0	1.82	0.00	0.00	0.10	0.30	-51.7
Mar..		C5	0.10	0.63	167.87	0.24
26...		C4	0.07	1.61	175.52
		C3	0.28	2.51	178.34	0.47
		C2	0.19	3.08	164.24	0.47	0.46	55.3
1995	8	C0	2.09	0.00	0.00	0.18	0.72	42.9
Oct..		C4	0.19	1.08	168.49	0.48
17...		C3	0.21	2.08	176.01	0.37
		C2	0.74	2.91	169.90	1.51	0.47	-72.6
		C1	0.15	3.45	192.01	0.76

^a Data at 5 GHz are ours and data at 8 GHz are from PK 97, data at 15.4 GHz, 22.2 GHz and 43 GHz are from Jorstad 2000.

^b Flux density in Jy.

^c r and θ are the polar coordinates of the center of the component relative to the presumed core C0. Polar angle is measured from north through east.

^d a and b are the FWHM of the major and minor axes of the Gaussian component.

^e Position angle of the major axis measured from north through east.

Table 2: the 5 GHz data are from our observation, the 8 GHz data are from PK 97, the 15 GHz, 22.2 GHz and 43 GHz data are from Jorstad 2000.

The model of beamed relativistic jet is the most straightforward and useful model to interpret the rapid variability found in some quasars; moreover it is commonly thought that gamma-rays are produced from inverse Compton scattering of synchrotron photons (for example, X-ray photons) by relativistic electrons in a beamed relativistic jet, so gamma-ray sources containing relativistic jets show evident apparent superluminal motion. The gamma-ray blazar 1611+343 is one of the sources displaying distinct apparent superluminal motion.

In fact, consider a blob of matter ejected from a stationary source at an angle to the sight line of the observer: only the component normal to the sight line could be detected. In the co-moving frame of the stationary source the angular displacement corresponds to a linear displacement:

$$dl = r S(t_e) d\theta, \quad (1)$$

where r is the radial coordinate of the source used in the Robertson-Walker line element, $S(t_e)$ is the cosmological scale factor corresponding to moment t_e . Obviously $dt_e = \frac{dt_0}{1+z}$, z being the redshift, and t_0 the initial time. The magnitude of the proper velocity v_{app} which is normal to the sight line in the source frame as determined by the observer is defined as

$$v_{\text{app}} = \frac{dl}{dt_e} = r S(t_e) \frac{d\theta}{dt_e} = \mu r S(t_0), \quad (2)$$

where $\mu = \frac{d\theta}{dt_0}$ is the apparent proper motion, using $\frac{\delta t_0}{S(t_0)} = \frac{\delta t_e}{S(t_e)}$, and the metric distance is defined as

$$d_m = r S(t_0) = \left(\frac{c}{H_0 q_0^2} \right) \left(\frac{q_0 z + (q_0 - 1) (\sqrt{1 + 2zq_0} - 1)}{1 + z} \right). \quad (3)$$

Including $\beta_{\text{app}} = v_{\text{app}}/c$ and practical units, a useful equation can be achieved as the following:

$$\beta_{\text{app}} = \left(\frac{47.2}{h q_0^2} \right) \times \left(\frac{\mu}{1 \text{ mas yr}^{-1}} \right) \times \left[\frac{q_0 z + (q_0 - 1) (\sqrt{1 + 2q_0 z} - 1)}{1 + z} \right] \quad (4)$$

(Kembhavi & Narlikar 1999). Introducing the angle between the bulk velocity and the sight line, ϕ , the observed transverse velocity of separation is related to the true velocity:

$$\beta_{\text{app}} = \frac{\beta \sin \phi}{1 - \beta \cos \phi} \quad (5)$$

(Pearson & Zensus 1987). The Doppler boosting factor is given by

$$\delta = [\Gamma (1 - \beta \cos \phi)]^{-1} \quad (6)$$

In terms of β_{app} from the superluminal motion data (Equation (4)) and δ estimated from the synchrotron self-Compton (SSC) model, we have, from Equations (4) and (5),

$$\Gamma = \frac{\beta_{\text{app}}^2 + \delta^2 + 1}{2 \delta}. \quad (7)$$

The SSC model assumes that the particles and magnetic field are in energy equipartition (Readhead 1994); so we have

$$\delta_{\text{eq}} = \left\{ [10^3 F(\alpha)]^{34} \left[\frac{1 - (1+z)^{-0.5}}{2h} \right]^{-2} (1+z)^{15-2\alpha} S_{\text{op}}^{16} \theta_{\text{d}}^{-34} (10^3 \nu_{\text{op}})^{-(2\alpha+35)} \right\}^{1/(13-2\alpha)}, \quad (8)$$

where $F(\alpha)$ is assumed to be 3.4 when α , spectral index, is selected as -0.75 . z is the redshift, S_{op} the observed peak flux density in Jy at the observed frequency ν_{op} in GHz. In particular, the angular diameter θ_{d} is $1.8 \theta_{\text{FWHM}}$ ($\theta_{\text{FWHM}} = (\theta_{\text{max}} \times \theta_{\text{min}})^{1/2}$) and $h = 1$ here. Observationally, the brightness temperature of an elliptical Gaussian component is given by

$$T_{\text{b}} = 1.77 \times 10^{12} (1 + z) \frac{S_{\text{op}}}{\theta_{\text{d}}^2 \nu_m^2} \text{K} \quad (9)$$

(Ghisellini et al. 1993). T_{b} of a synchrotron source was once used to identify beamed components. When T_{b} is above 10^{12} K, the radiation energy will dominate in the source, the inverse Compton scattering enhances greatly. In company with a great deal of synchrotron photons being scattered into even higher-energy photons, the source will lose a vast amount of energy and cool down rapidly. So T_{b} of a radio source generally does not exceed 10^{12} K in the absence of continuous supply of energy.

Figure 2 shows the EVPA (electric vector position angle) distribution in the jet (the magnetic field is normal to the EVPA). Since Shanghai and Urumqi has only single-polarization equipment, the P VLBI data were produced by the European antennas. The baselines between the European antennas whose data are used to make the P VLBI map are shorter than those whose data are used to make the I VLBI map, the beam of the P VLBI map is much larger than the beam of the I VLBI map. The direction of the jet is by and large parallel to the magnetic field in Fig. 2. We detected polarization peak at about 3 mas south of the core, where we consider the jet to bend on the mas scale.

The spectral index of C0 is -0.05 , which indicates a flat and inverted spectrum. The spectrum of component C3 is rather steep. The blazar 1611+343 is a flat spectrum radio source with a mean spectral index $\alpha = -0.04$ (PK 97). Its radio variability has been monitored and there was a prominent outburst in 1993 and peaks in 1995; optical variability reported an outburst between October 1986 and March 1987 (Tornikoski et al. 1994). The total flux variation of 1611+343 in time is shown in Fig. 3. It reveals prominent activity peaks in 1990 and 1996. The flux increased in all the three bands between 1989 and 1999. C4 and C5 were ejected in December 1991 and May 1994, respectively (PK 97). It seems that a correlation exists in time between ejection of component and flux enhancement. (Fig. 3).

4 DISCUSSION ON THE CURVED JET

Curved jets are common in AGNs. An interpretation of the curved jet in 1611+343 was presented in PK 97 that each component was ejected from the core with its own independent position angle, and then moved straight out from the core along a uniform and common trajectory.

The VLA image revealed that 1611+343 is an aligned source at arcsecond scale. While our mas-scale data show jet bending at about 3 mas south of the presumed core. Moreover our P VLBI map shows polarization peaks where the jet bent eastwards. Here we tend to interpret the curving of the jet in 1611+343 with a shock wave model. In this scenario a moving jet component is hindered by the ambient medium, (for instance, dense cloud) around 3 mas south of the core. The interaction between the jet component and ambient medium produces a stationary shock wave at the interface. The jet component is deflected in the interface and bends eastwards. The continued motion of the jet components is not clear for lack of enough data at large scale. To further study the jet configuration of 1611+343, we need multi-frequency data to give the configuration at different scales.

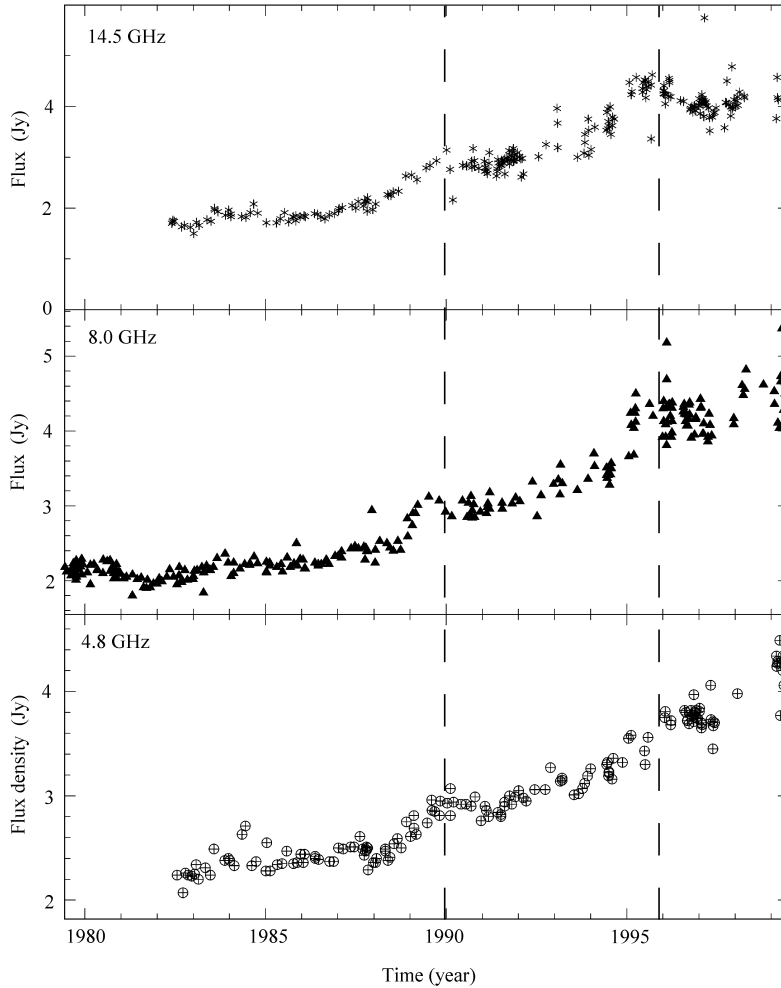


Fig. 3 The total flux densities vary with epochs at 4.8 GHz, 8.0 GHz and 14.5 GHz. The data are from the University of Michigan Radio Astronomy Observatory. The vertical lines denote the peaks of enhanced flux.

Continued VLBI monitoring of 1611+343 at lower frequencies is important to reveal the source configuration at large scale, and to help to further interpret the motion of jet components.

5 CONCLUSION

We present the I VLBI image of 1611+343 at 5 GHz and report on the detection of apparent superluminal motion in three components C5, C2 and C3. The apparent superluminal velocities of these three components verify the relativistic bulk motion in the source. The physical parameters of the jet components also support the assertion that components moving at superluminal

velocity exist in 1611+343. The geometry of the jet is mapped and a curved jet is obtained. The P VLBI image displays the EVPA distribution in the jet and reveals polarization peak where jet bends at mas scale. A stationary shock model is introduced to describe the eastward bending of the jet at mas scale.

Acknowledgements This research was supported by the National Natural Science Foundation of China (19973103) and the National Climbing Program. The authors are grateful to the staff of the EVN for the support of the observing projects.

References

- Bondi M. et al., 1996, *A&A*, 308, 415
Conway J. E., Murphy D. W., 1993, *ApJ*, 411, 89
Ghisellini G. et. al., 1993, *ApJ*, 407, 65
Hardee P. E., 1987, *ApJ*, 318, 78
Hewitt A., Burbidge G., 1989, *ApJS*, 69, 1
Jorstad et al., 2000, *ApJS*, in press
Linfield R. P., 1981, *ApJ*, 250, 464
Lister M. L., Marscher A. P., 1998, 702, 719
Kaastra J. S., Roos N., 1992, *A&A*, 254, 96
Kembhavi A. K., Narlikar J. V., 1999, In: A. K. Kembhavi, J. V. Narlikar, eds., *Quasars and Active Galactic Nuclei: An Instruction*, p.53
Murphy D. W., Browne I. W. A., Perley R. A., 1993, *MNRAS*, 264, 298
Padrielli L. et al. 1986, *A&A*, 165, 53
Padrielli L., Eastman W., Gregorini L. et al., 1991, *A&A*, 249, 351
Piner B. G., Kingham K. A., 1997, *ApJ*, 479, 684 (PK 97)
Romney J. D. et al., 1984, *A&A*, 135, 289
Rusk R. E., 1988, Ph.D. thesis, Univ. Toronto
Rusk R. E., Seaquist E. R., 1985, *AJ*, 90, 30
Steffen W., Zensus J. A., Krichbaum T. P. et al., 1995, *A&A*, 302, 335
Tornikoski M., Valtaoja E., Teräsanta H. et al., 1994, *A&A*, 289, 673